

## Study of Implementation of Led Using Cads Based Quantum Dot

Dr Jyotsna Chauhan\*, Vishal Bhopche

\*HOD Department of Nanotechnology, Rajiv Ganhi Technical University, Bhopal (M.P.), India

Corresponding Authors: Dr Jyotsna Chauhan

---

**Abstract:** The narrow tunable emission spectra and high photo-luminescence efficiency make QDs potentially the most practical candidates for making quantum-dot light emitting devices. In the last decade or more, a considerable amount of research has been focused on developing highly efficient QD-LEDs.[1-4] Quantum dot led have great potential for being used for energy efficient high colour quality thin-film display and solid-state lighting. The wide absorption spectrum, band gap tunability and cheap solution processibility make quantum-dot a promising candidate for solar cells as well. Additionally, solution-processed quantum dot allows processing onto light-weight exible substrates through spin coating, spray-coating, reel-to-reel printing and inkjet printing which can potentially reduce the fabrication and packaging cost[5].

---

Date of Submission: 04-04-2018

Date of acceptance: 19-04-2018

---

### I. INTRODUCTION

The potential of QDs for application in full-colour video, solid-state lighting, next-generation solar cells, detector arrays, and lasers make them one of the most attractive candidates for photonic applications

**Scherrer formula:** Scherrer equation is used to calculate the Nano crystallite size ( $L$ ) by XRD radiation of wavelength  $\lambda$  (nm) from measuring full width at half maximum of peaks ( $\beta$ ) in radian located at any  $2\theta$  in the pattern.

$$L = \frac{K\lambda}{\beta \cdot \cos\theta}$$

where  $\lambda$  - is the X-ray wavelength in nanometre (nm)

$\beta$ - Is the peak width of the diffraction peak profile at half maximum height resulting from small crystallite size in radians

$K$ - Is a constant related to crystallite shape, normally taken as 0.9[10]

**Uniform strain:** If ' $\Delta d$ ' is the change in the  $d$ -spacing in the stressed quantum dot relative to the undeformed grain of bulk material, the corresponding uniform strain is given by-

$$\kappa = c \left( \frac{d_f - d_0}{d_0} \right) = c \frac{\Delta d}{d_0}$$

Where,  $c$  is a material dependent constant[11].

**Non-uniform strain ( $\eta$ ) with particle size using the Hall equation:**

$$\beta \frac{\cos\theta}{\lambda} = \frac{1}{t} + 2\eta \frac{\sin\theta}{\lambda}$$

Where, ' $\lambda$ ' is the wavelength of x-ray used for scattering experiment and ' $t$ ' is the particle size and  $\beta$  is the line broadening[12].

---

## II. STRUCTURAL ANALYSIS

Figure 1 shows typical X-ray diffraction patterns of the three CdS samples deposited without (a) and in presence of the surfactant (b and c) [13]. A systematic decrease in the size of the particles in the CdS nanoparticle could be achieved by increasing the surfactant to thiourea ratio. Typical X-ray diffraction pattern exhibited by typical CdS nanoparticle grown using surfactant to thiourea ratio of (b) 0.13 and (c) 0.15 has also been shown in Figure 1. A systematic broadening of the line widths and weakening of the intensities at higher angles with increasing surfactant concentration was seen in Figures 1(b and c). The successive broadening of the XRD reflections resulting from nanocrystalline CdS sample b and c implied a concomitant reduction in particle size for increasingly higher concentration of mercaptoethanol employed during synthesis. Because of the preferential orientation and the particle size related broadening, the X-ray diffraction peaks from the higher index planes of the CdS nanoparticle considerably broaden and merge with each other while simultaneously decreasing in intensity as could be seen from Figures 1(b and c). To ascertain the peak positions and  $d$ -values from the broadened reflexes, we deconvoluted the peaks assuming a Gaussian line shape. The results of the deconvolution have also been shown in the figure by dotted lines. The observed peak positions, corresponding  $d$ -values and Miller plane assignments along with standard JCPDS[14] data have been summarized in Table I. The average particle size calculated from the Scherrer's broadening[6-9] of the X-ray diffraction was obtained as 2.4 nm and 1.7 nm for sample b and c respectively.

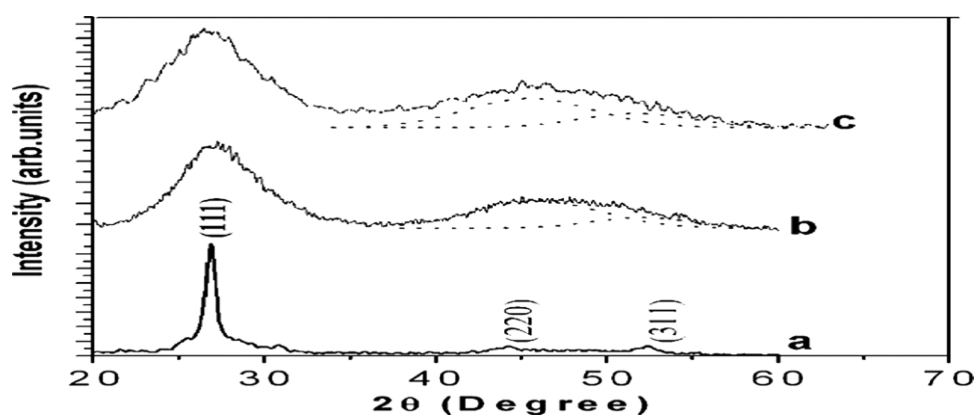


**Fig.1** XRD spectra of (a) polycrystalline CdS, CdSQD grown using surfactant to thiourea ratio of (b) 0.13 and (c) 0.15. The deconvoluted (220) and (311) peaks have also been shown by dotted curve [23].

From the Figure.1 it is clear that in sample a,b and c most prominent peak obtained corresponds to (111) plane. Some peak also obtained corresponds to (220) and (311) but there intensities are not at that much level as we desire. From the most prominent peak we can calculate some useful parameter like grain size, FWHM, inter planner distance ( $d$ ) and some other various useful parameters. Here we have compare the standard  $d$  values with observed by our calculation. Standard values are obtained from JCPDS data book. Now we can calculate the values of grain size from scherrer equation that come in the range from 1-10 nanometer for our desired peak. The grain size in 1-10 nanometer is also useful for calculation of strain of partical. So here we also calculate the average strain and nonuniform strain.

From the Figure 1 it is clear that in case of sample a, the observed profile is characterized by a sharp diffraction peak at  $2\theta=26.83^\circ$  along with two other peaks at the location  $2\theta=44.33^\circ$  and  $52.31^\circ$  but the intensities of these two peaks are not at that level as we required. These peaks are corresponds to  $d$  values  $3.31 \text{ \AA}$ ,  $2.04 \text{ \AA}$  and  $1.76 \text{ \AA}$  respectively. From these peaks we can obtained FWHM, it is clear that whenever grain size reduces to 21nm to 1.7nm the peaks are going to be broaden. We have observed FWHM for grain size 21nm, 2.4nm and 1.7nm are  $0.388^\circ$ ,  $3.40^\circ$  and  $4.80^\circ$  respectively. The observed XRD spectra for sample a signify deposition of a polycrystalline phase of CdS. The observed peaks are contributed by the (111), (220) and (311) planes of the cubic phase of CdS. Comparison of the experimentally observed peak intensities with the corresponding standard values also indicated preferred growth of (111) planes the experimentally determined peak position, corresponding  $d$ -values and miller plane assignment for this film have been summarized in table 1

**Table 1-**A summary of the X-ray diffraction data for the polycrystalline CdS as well as nanocrystalline-CdS films with different size [13].

Sample	Grain size(nm)	2 (Deg.)	FWHM (degree)	d values(A°)		Miller plane (hkl)	Phase assignment
				Standard	observed		
a.	21.0	26.83	0.388	3.36	3.32	(111)	Cubic
		44.33	0.408	2.06	2.04	(220)	Cubic
		52.31	0.421	1.75	1.76	(311)	Cubic
b.	2.4	26.85	3.40	3.36	3.31	(111)	Cubic
		45.49	3.58	2.06	1.99	(220)	Cubic
		51.71	3.67	1.75	1.76	(311)	Cubic
c.	1.7	26.90	4.80	3.36	3.31	(111)	Cubic
		45.90	5.70	2.06	1.98	(220)	Cubic
		52.70	5.21	1.75	1.75	(311)	Cubic

**Table 2-** A summary of the avg. strain and nonuniform strain for different size of CdS QD:

Sample	Grain size(nm)	2 (Degree)	Avg. strain	Nonuniform strain
a.	21.0	26.83	$7.07 \times 10^{-3}$	$-1.605 \times 10^{-3}$
b.	2.4	26.85	$61.96 \times 10^{-3}$	$-14.25 \times 10^{-3}$
c.	1.7	26.90	$87.30 \times 10^{-3}$	$-10.541 \times 10^{-3}$

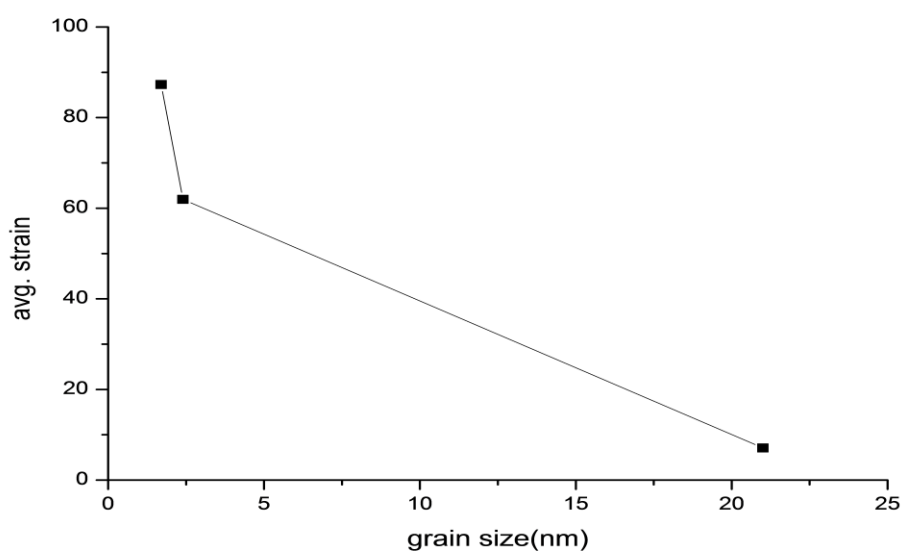


**Fig. 2** Graph between avg. strain and grain size

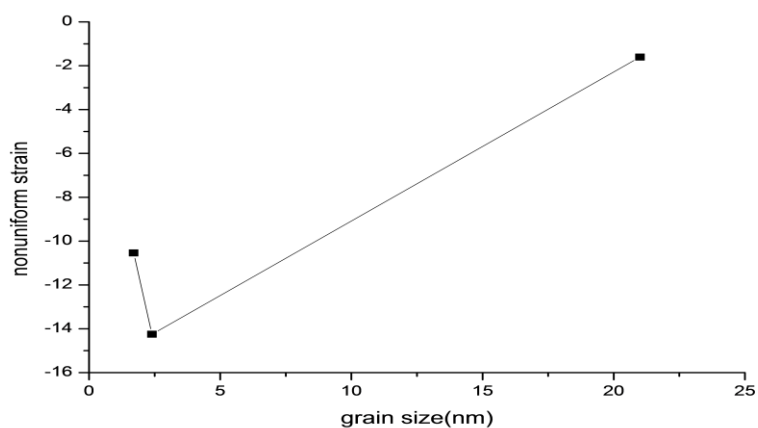


**Fig. 3** Graph between grain size and non-uniform strain

as we seen in graph fig.2 and fig. 3 as the size of grain reduces the strain increase. The strain generally occurs only in those nanoparticle whose size is mostly in between 1-10 nanometer.

### III. UV-VISIBLE ABSORPTION SPECTROSCOPY

The radiation from normal hot solids is made up of many wavelengths and the energy emitted at any particular wavelength depends largely on the temperature of the solid and is predictable from probability theory. The curves in Figure 4 show the energy distribution for a tungsten filament at three different temperatures. Such radiation is known as 'black body radiation'. Note how the emitted energy increases with temperature and how the wavelength of maximum energy shifts to shorter wavelengths. More recently it has become common practice to use a variant of this - the tungsten-halogen lamp. The quartz envelope transmits radiation well into the UV region. For the UV region itself the most common source is the deuterium lamp and a UVVisible spectrometer will usually have both lamp types to cover the entire wavelength range.

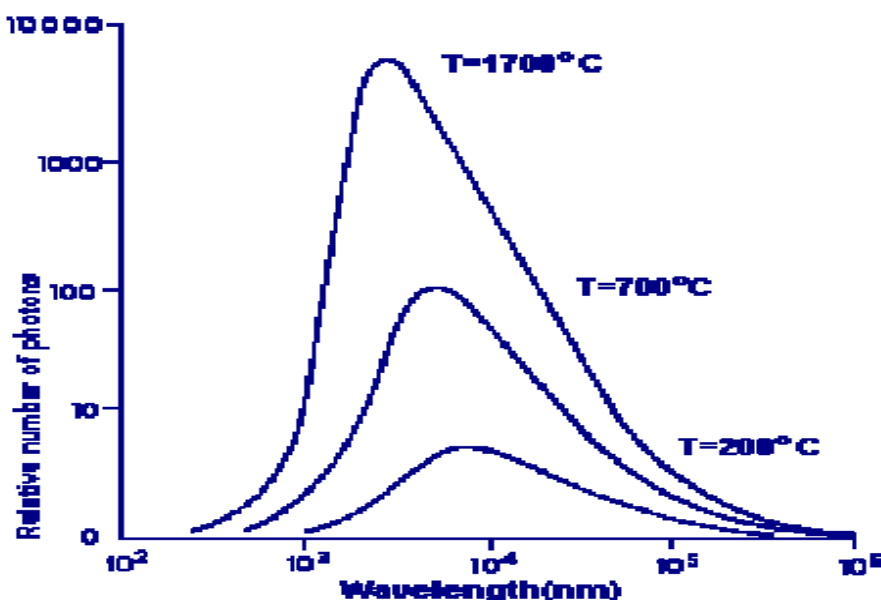


**Fig 4** Tungsten filament radiation [23]

For ultraviolet and visible wavelengths, one should expect from this discussion that the absorption spectrum of a molecule (i.e., a plot of its degree of absorption against the wavelength of the incident radiation) should show a few very sharp lines. Each line should occur at a wavelength where the energy of an incident photon exactly matches the energy required to excite an electronic transition.

In practice it is found that the ultraviolet and visible spectrum of most molecules consists of a few humps rather than sharp lines. These humps show that the molecule is absorbing radiation over a band of

wavelengths. One reason for this band, rather than line absorption is that an electronic level transition is usually accompanied by a simultaneous change between the more numerous vibrational levels. Thus, a photon with a little too much or too little energy to be accepted by the molecule for a 'pure' electronic transition can be utilized for a transition between one of the vibrational levels associated with the lower electronic state to one of the vibrational levels of a higher electronic state. If the difference in electronic energy is 'E' and the difference in vibrational energy is 'e', then photons with energies of E, E+e, E+2e, E-e, E-2e, etc. will be absorbed. Furthermore, each of the many vibrational levels associated with the electronic states also has a large number of rotational levels associated with it. Thus a transition can consist of a large electronic component, a smaller vibrational element and an even smaller rotational change. The rotational contribution to the transition has the effect of filling in the gaps in the vibrational fine structure.

In addition, when molecules are closely packed together as they normally are in solution, they exert influences on each other which slightly disturb the already numerous, and almost infinite energy levels and blur the sharp spectral lines into bands. These effects can be seen in the spectra of benzene as a vapour and in solution. In the vapour, the transitions between the vibration levels are visible as bands superimposed on the main electronic transition bands.

The typical absorption spectra of as prepared poly as well as two Nano crystalline Q-CdS samples, having particle size 21.0 nm, 2.4 nm and 1.7 nm respectively have been shown in Figure 5 [23].

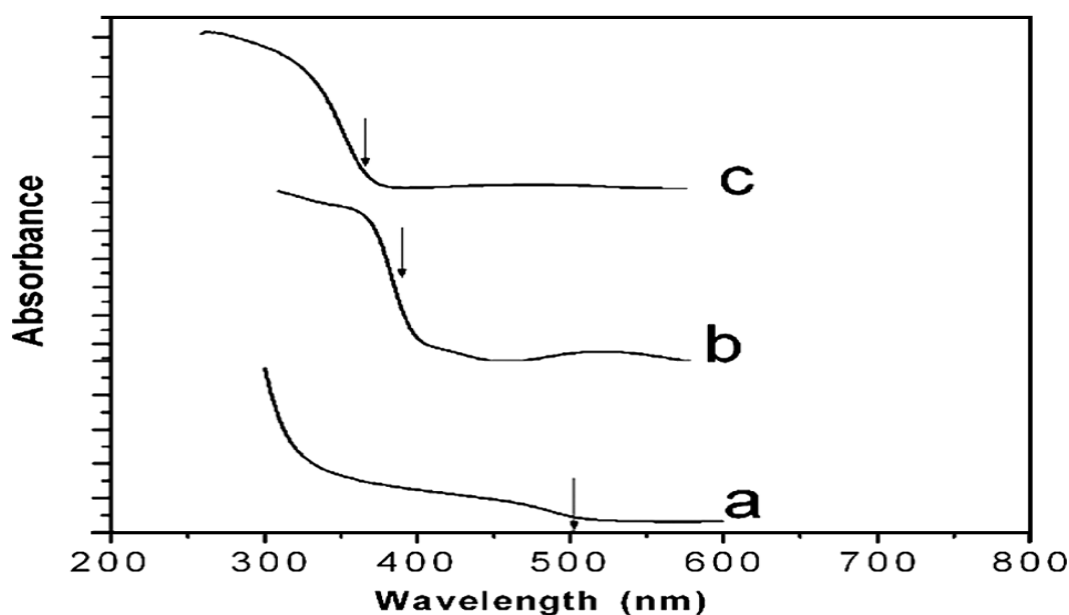


Fig. 5 Optical absorption spectra [23]

The spectral positions of the optical absorption edges for the CdS samples were determined from the second order derivative of the observed spectra. These have also been marked in the figure. Sharp onset of absorption at fundamental absorption edge could be seen in all the samples. The polycrystalline CdS film exhibited an absorption edge at 504 nm (2.46 eV), which is close to the value of the band gap for the bulk specimen. The absorption edge however, shifted to the lower wavelength side for Nano crystalline CdS QD. The fundamental absorption edge was seen to gradually shift towards shorter wavelength side from 394 nm (b) to 365 nm (c) as the particle size decreased from 2.4 nm to 1.7 nm [13]. The observed absorption edges for the two nano crystalline samples corresponded to transitions from the levels 1Sh (highest occupied molecular orbital-HOMO) to 1Se (lowest unoccupied molecular orbital-LUMO) in CdS quantum dots. In fact, we have observed a systematic size dependent blue shift in the absorption edges with the decrease in particle size of Q-CdS samples. These Q-dots were synthesized using increasingly higher mercaptoethanol to thiourea ratio in the growth matrix. The observed dependence of absorption edge on the particle size of the Nano crystalline CdS films has been pictorially represented in Figure 6 [13].

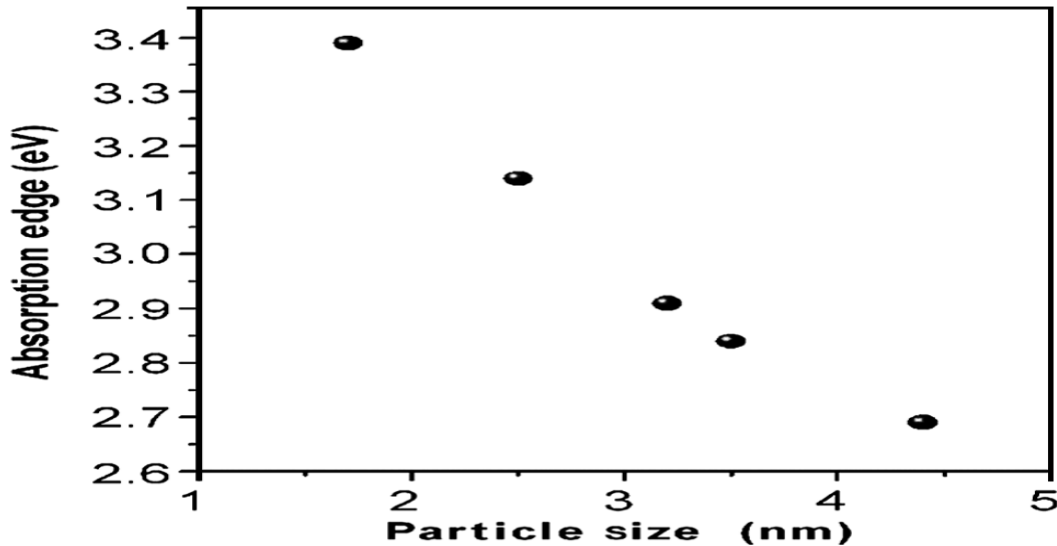


Fig. 6 Observed dependence of the absorption edge for Nano crystalline Cds QD [23]

#### IV. EMA APPROXIMATION CALCULATION

Explained qualitatively by considering a particle-in-a-box like situation, where the energy separation between the levels increases as the dimensions of the box are reduced. The variation in the electronic structure of Nano crystalline as a function of its size can be explained by various theoretical approaches. We have attempted to correlate the observed blue shift with the results calculated by using the effective mass approximation (EMA) as well as the tight binding (TB) model. Using EMA Brus, proposed following relationship for the particle size dependent energy gap:

$$E(R) = E_g + \frac{\hbar^2}{2} \left( \frac{1}{m_e^*} + \frac{1}{m_h^*} \right) \frac{\pi^2}{R^2} - 1.786 \frac{e^2}{\epsilon R} - 0.248 E_{Ry}^* \quad (1)$$

Where  $E_g$  is the bulk band gap and  $R$  the particle diameter in nm. The second term in Eq.(1) is the kinetic-energy term containing the effective masses,  $m_e^*$  and  $m_h^*$ , of the electron and the hole, respectively. The third term arises due to the Coulomb attraction between the electron and the hole, and the fourth term is due to the spatial correlation between the electron and the hole, which is generally small, compared to the other two terms.

In the effective mass approximation EMA, can use the energy position to estimate the average particle size. The Coulomb potential and polarization energy were small compared to electron- hole confinement kinetic energy, so that this equation can be approximately written as:

$$E(R) = E_0 + \frac{\hbar^2 \pi^2}{2R^2} \left( \frac{1}{m_e} + \frac{1}{m_h} \right)$$

Where  $E_0 = 2.42$  eV,  $m_e = 0.21m_0$ ,  $m_h = 0.80m_0$ , and  $m_0$  is the free electron mass.

Table 3 A summary of grain size and their respective band gap by EMA method:

Sample	Grain size (nm)	E(R) (eV)
a.	21.0	2.425
b.	2.4	2.616
c.	1.7	3.20

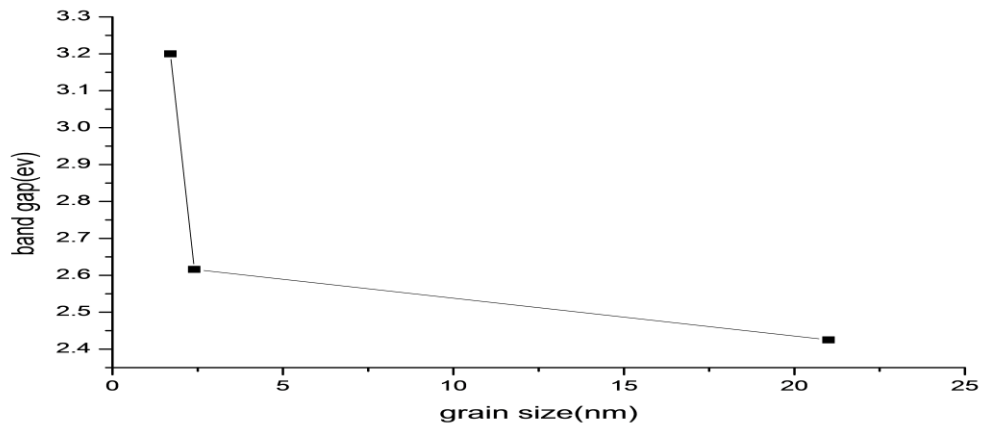


Fig. 7 graph between band gap and grain size

### V. TIGHT BINDING APPROACH

Tight binding approach is based on a simple physical picture in terms of the atomic orbitals and hopping interactions defined over a predetermined range and has been employed by a number of researchers for calculating a size dependent shift in absorption edge. Using tight binding model, proposed the following relationship for the energy shift

$$\Delta E_g = a_1 e^{-R/b_1} + a_2 e^{-R/b_2} \quad (2)$$

$E_g$ , the band gap shift for any system can be calculated for any size of the Nano crystallites with the knowledge of parameters  $a_1$ ,  $b_1$ ,  $a_2$ , and  $b_2$ . Taking the values of the parameters  $a_1=2.65$ ,  $b_1=7.61$ ,  $a_2=1.90$ , and  $b_2=23.50$ , the energy shifts were calculated for our samples.  $R$  is the particle size of the Nano crystallite in Å.

Table 4- A summary of grain size and their respective band gap by TBM method:

Sample	Grain size (nm)	$E_g$ (eV)
a.	21.00	4.549
b.	2.4	4.55
c.	1.7	4.56

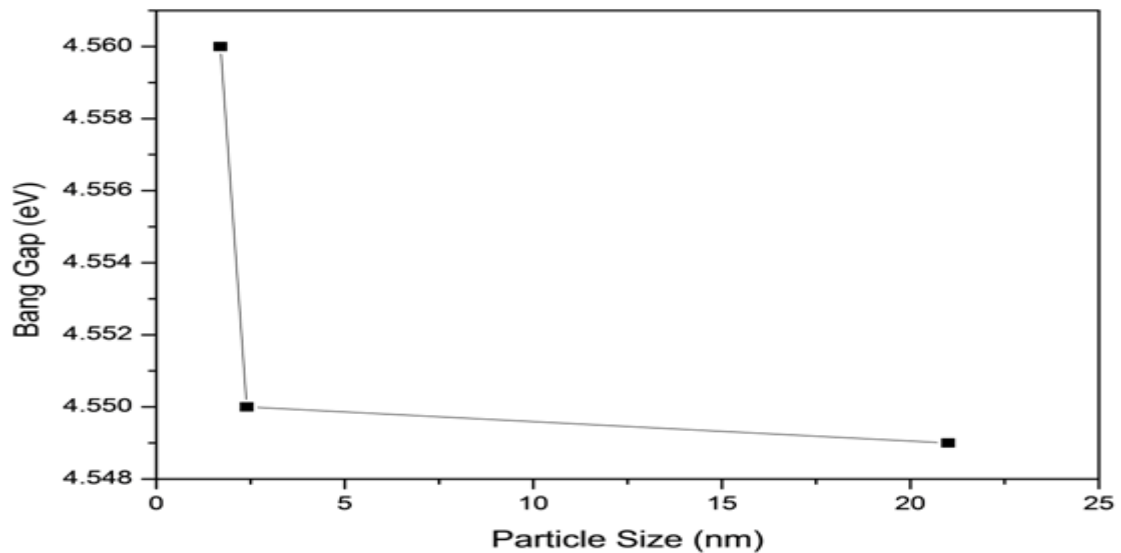


Fig. 8(a) graph between band gap and grain size

### VI. HYPERBOLIC BAND MODEL

The hyperbolic band model is based on the assumption that lowest lattice excitation of the semiconductor involves electron transfer from  $S^{2-}$  to  $Cd^{2+}$  at a cost in energy equal to the bulk band gap. Further it is assumed that only two bands are important at the  $\Gamma$  point to calculate band gap energy between highest occupied valence band and the lowest unoccupied conduction band. On the basis of above assumptions the following analytical formula has been derived for band gap energy

**Table 5-** A summary of grain size and their respective band gap by HBM method:

Sample	Grain size (nm)	E(R) (ev)
a.	21.00	2.397
b.	2.4	2.605
c.	1.7	2.883

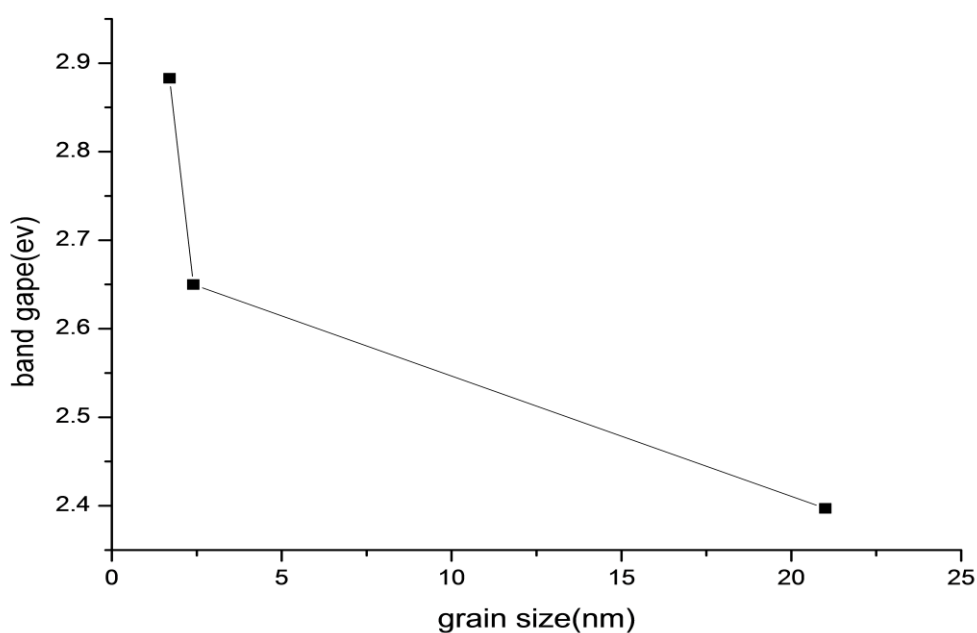


Fig.8(b) graph between grain size and band gap

**Table 6-** Comparison of band gap obtained by different method for CdS nanoparticle:

Sample	Grain size	Band gap		
		EMA	TBM	HBM
a.	21	2.425	4.549	2.397
b.	2.4	2.616	4.55	2.605
c.	1.7	3.20	4.56	2.883



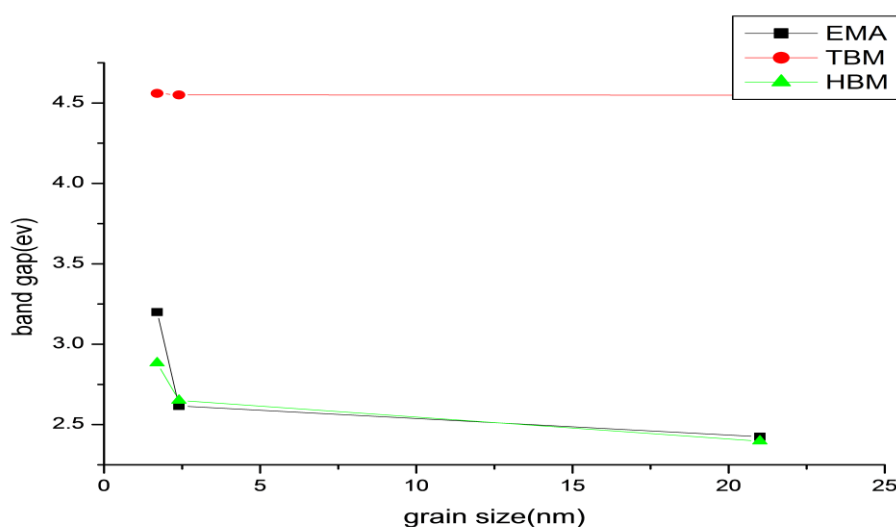


Fig. 9 combine graph for EMA TBM AND HBM

As we seen in the graph plotted between grain size and band gap of the material, whenever size reduces to 21nm to 1.7nm the band gap of material increases. This property very important for any material which can be used for as a light emitting element. These band gap are calculated by three different methods namely EMA, TBM and HBM. From the above discussion it is clear that HBM method is not suitable for our calculation. Band gap in EMA and TBM is very close but in HBM it is not occur properly as we desire.

## VII. CONCLUSION

From the above discussion it can be concluded that whenever size of the particle reduces towards the nanolevel their band gap increases. Strain also increases in the range if we able to restrict particle size between 1 to 10 nm. From the XRD analysis we find particle size in our sample 21nm for bulk CdS and 2.4 and 1.7 nm for CdS quantum dot by applying appropriate capping agent during synthesis process. We can find variation in band gap by UV Visible absorption spectroscopy. Here we use three methods for calculation of band gap of CdS quantum dot; the methods namely are EMA, TBM and HBM. The variation in band gap by changing the grain size we can observed by graph plotted between grain size and band gap. From the graph it is very clear that the whenever the grain size reduces band gap increases. These properties are very important for light emission of any material. The optical absorption studies revealed that the observed absorption edges in the Nano crystalline samples exhibited a blue shift due to the quantum confinement effect. The blue shift in the absorption edge was shown to be dependent on the size of the CdS nanoparticle. Whenever size reduces they can absorb light of small wavelength, that's why blue shift occur whenever size reduces to nanometre. The photoluminescence emission spectroscopy of the cadmium sulfide films has also been investigated. It is shown that the CdS QD exhibit intense photoluminescence as compared to the large grained CdS nanoparticle. The effect of quantum confinement also manifested as a blue shift of photoluminescence emission. From the discussion it is also clear that whenever size of QD reduces they absorb radiation of small wavelength that means the frequency of emitted light increases as size reduces. These all properties are makes QD is very useful for implementation of LED.

## REFERENCES

- [1] L.E. Brus (2007) "Chemistry and Physics of Semiconductor Nanocrystals" (PDF). Retrieved 7 July 2009.
- [2] D.J. Norris (1995). "Measurement and Assignment of the Size-Dependent Optical Spectrum in Cadmium Selenide (CdSe) Quantum Dots, PhD thesis, MIT". hdl:1721.1/11129.
- [3] C. B., Murray, Kagan, C. R.; Bawendi, M. G. (2000). "Synthesis and Characterization of Monodisperse Nanocrystals and Close-Packed Nanocrystal Assemblies". *Annual Review of Materials Research* 30(1):545–610. Bibcode:2000AnRMS..30..545M. doi:10.1146/annurev.matsci.30.1.545.
- [4] "Nanotechnology Information Center: Properties, Applications, Research, and Safety Guidelines". American Elements.

- [5] C. Sullivan, S.; Steckel, J. S.; Woo, W.-K.; Bawendi, M. G.; Bulović, V. (2005-07-01). "Large-Area Ordered Quantum-Dot Monolayers via Phase Separation During Spin-Casting". *Advanced Functional Materials* 15 (7): 1117–1124. doi:10.1002/adfm.200400468. ISSN 1616-3028.
- [6] B. D. Cullity, "Elements of X-Ray Diffraction", Reading, MA: Addison Wesley, 1956.
- [7] B. E. Warren, "X-Ray Diffraction", Ed. 2, reprint, illustrated, Pub. Courier Dover Publications, 1969, ISBN-0486663175, 9780486663173.
- [8] C. Suryanarayana and M. G. Norton, "X-Ray Diffraction: A Practical Approach", Ed. Illustrated, Pub. Springer, 1998, ISBN- 030645744X, 9780306457449.
- [9] W. Massa, "Crystal Structure Determination", Ed. 2, illustrated, Pub. Springer, 2004, ISBN-3540206442, 9783540206446. pp.124
- [10] H. Klug and L. Alexander, "X-Ray diffraction procedure for Polycrystallite and Amorphous material," 2<sup>nd</sup> edition, John Wiley and Sons, New York, 1974.
- [11] J. Mazhar, A. K. Shrivastava, N. V. Nandedkar, R. K. Pandey, "Strained ZnSe Nanostructure Investigations by X-ray, AFM, TEM and Optical Absorption Luminescence Spectra", *Nanotechnology*, 15, 572-580 (2004).
- [12] D. Kaushik, Thesis "Studies on Low Dimensional II-VI Semiconductor Compounds", B. U. Bhopal (2007).
- [13] D. Kaushik Study of Self-Organized CdS Q-Dots, Madhulika Sharma, A. B. Sharma, and R. K. Pandey Materials Research Lab, Department of Physics, Bhopal University, Bhopal 462026, India
- [14] Powder Diffraction File, Joint Committee on Powder Diffraction Standards, Pennsylvania, USA, 1974, card 10-0454.

IOSR Journal of Pharmacy (IOSR-PHR) is UGC approved Journal with SI. No. 5012

Dr Jyotsna Chauhan "Study of Implementation of Led Using Cads Based Quantum Dot." IOSR Journal of Pharmacy (IOSRPHR), vol. 8, no. 04, 2018, pp. 85-94